

Spatially resolved 2-D attenuation image of a semi-infinite non-homogeneous tissue from diffuse reflectance

Jorden Tse and Lian-Kuan Chen

The Chinese University of Hong Kong, Hong Kong, China

ABSTRACT

Optical properties of biological tissue such as reduced scattering and absorption coefficients can be determined from the temporal or spatial reflectance curve of the diffusion process. Owing to its non-homogenous nature, the assumption of uniform optical parameters may not be valid in practice. We propose a new scheme to resolve the optical effective attenuation profile from the spatial reflectance curve of a non-homogeneous tissue. The algorithm reconstructs the linear attenuation profile along the line of measurement, rather than giving one single value for the coefficient for each reflectance curve. The technique was applied to the reconstruction of a 2-dimensional attenuation image.

Keywords: Diffuse Reflectance, Light Scattering, Biomedical Application

I. INTRODUCTION

When light propagates through a biological tissue, photons are absorbed, scattered, reflected or refracted. The absorption of a photon and the way energy transfers are related to the nature of the matter interacted. Information about the physical density and chemical concentration of the tissue can be deduced from the observation of the spatial distribution and intensity of diffused light. For instance, oximeter uses the absorption properties of red and infra-red light to give the hemoglobin composition and oxygen saturation in blood [1]. Diffusion theory model [2] and Monte Carlo (MC) simulation [3] give a good approximation on the distribution of diffused light. In practice, we are interested in the chemical and physical properties of biological tissue, which can be estimated from the optical properties of that tissue. Using the inverse of the theory and simulation, the reduced scattering and absorption coefficients can be estimated from the measured diffuse reflectance or transmittance, using photo-detectors [4] or CCD camera [5] where the diffuse reflectance is a spatial [6] or temporal [7, 8] impulse response. In [6], the optical image of muscle oxygenation is obtained by multiple optical probes with multiple optical detectors in each probe. Oxygenation distribution is resolved spatially by using an array of light sources and detectors. This technique is also commonly used in functional near infrared image on the brain cortex [9, 10].

Biological tissue is non-homogenous in nature. By using multiple probes as in [6], 2-dimensional (2-D) reconstruction of optical properties of biological tissue can be obtained. However, the size of the probes limits the resolution of the reconstruction. Besides, it is commonly assumed that the tissue has uniform optical properties between the light source and detector of the probe and therefore, this creates a problem when some hetero-structures, such as blood vessels, are located between the light source and detector. The blood vessel, which has high red light absorption, may lead to erroneous calculation of the absorption and scattering value. In other words, the optical non-uniformity of tissue causes the diffuse reflectance curve deviating from that obtained by the solution of diffusion theory or Monte Carlo simulation. In this paper, we propose a new scheme to resolve the optical effective attenuation profile from the spatial reflectance curve of a non-homogeneous tissue. By capturing the diffuse reflectance in relatively high resolution using a CCD camera and by analyzing the spatial reflectance curve, we can resolve the spatial optical property variations, rather than just a single value, along a line originating from the light source. The reflectance curve describes the reflectance (R_d) at distance from the light source (r). At any specific distance r_0 , it is possible to resolve the absorption property at r_0 by assuming the optical properties in the section from $r_0 - \Delta r$ to $r_0 + \Delta r$ are uniform for a small Δr . Hence, we will show that it is possible to resolve the attenuation for every point on the curve, and therefore the attenuation profile along r can be obtained.

The paper is organized as follows. In the next section, the proposed algorithm to resolve the attenuation profile of a non-homogeneous medium is presented. The validation and experimental results using the algorithm are shown in

section III. We demonstrate the feasibility to resolve the 2-D attenuation profile in details. Finally, section IV concludes this paper.

II. MODEL AND ALGORITHM

The diffused reflectance R_d of light scattering in homogenous medium with absorption coefficient μ_a and reduced scattering coefficient μ_s' at distance r can be determined by the diffusion theory as in equation (1) [2]:

$$R_d(r) = a' \frac{z'(1 + \mu_{eff} \rho_1) \exp(-\mu_{eff} \rho_1)}{4\pi\rho_1^3} + a' \frac{(z'+4D)(1 + \mu_{eff} \rho_2) \exp(-\mu_{eff} \rho_2)}{4\pi\rho_2^3} \quad (1)$$

where $a' = \mu_s' / (\mu_s' + \mu_a)$, $D = [3(\mu_a + \mu_s')]^{-1}$, $\mu_{eff} = \sqrt{\mu_a/D}$, $z' = (\mu_a + \mu_s')^{-1}$, $\rho_1 = \sqrt{r^2 + z'^2}$ and $\rho_2 = \sqrt{r^2 + (z'+4D)^2}$. Although it is possible to resolve the effective attenuation coefficient μ_{eff} from (1), it is difficult to obtain a closed-form solution for μ_{eff} . Therefore, we approximate time-independent diffuse reflectance in the form of

$$R_d'(r) = k_1 r^{-k_2} \exp(-k_3 r) \quad (2)$$

with some positive constants k_1 , k_2 and k_3 . Figure 1 shows the curve fitting on the diffuse reflectance from an MC simulation with $\mu_a=0.1$ and $\mu_s'=10$. The fitted empirical formula using (2) is

$$R_d'(r) = 0.0650 r^{-2.217} \exp(-1.735r) \quad (3)$$

Comparison of Empirical Formula and MC Simulation

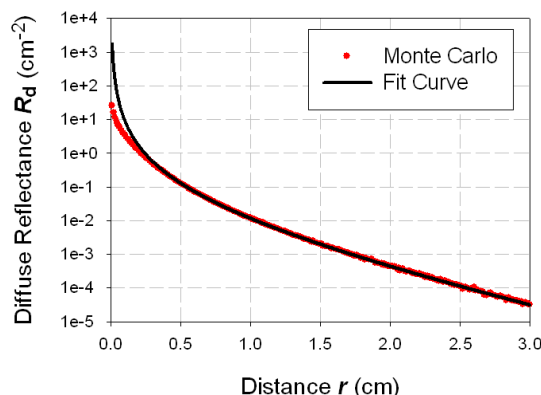


Figure 1) MC simulation result and the fitted curve of the empirical formula

From the comparison with the diffuse reflectance calculated from the MC simulation, the approximation of equation (2) is only invalid when r is small. This suggests that for points with a sufficient large r , an empirical formula in the form of equation (2) can be used to describe the diffusion curve. Deriving from (2), the value of k_2 and k_3 as a function of source-detector distance r_0 can be expressed as:

$$k_2(r_0) = r_0^2 \left. \frac{d^2 \ln R_d}{dr^2} \right|_{r=r_0} \quad (4)$$

$$k_3(r_0) = \left. \frac{d \ln R_d}{dr} \right|_{r=r_0} - r_0 \left. \frac{d^2 \ln R_d}{dr^2} \right|_{r=r_0} \quad (5)$$

Equation (4) and (5) reveal that the values of $k_2(r_0)$ and $k_3(r_0)$ only depend on the first and second derivatives at r_0 . The value of $\left. \frac{d \ln R_d}{dr} \right|_{r=r_0}$ and $\left. \frac{d^2 \ln R_d}{dr^2} \right|_{r=r_0}$ can be found by linear and quadratic regressions on the neighboring points

within $r_0 \pm \Delta r$. With $r_0=2.0$ and $\Delta r=0.2$, the relation between k_3 and μ_{eff} is obtained by varying the value of μ_a and μ_s' and is plotted in Figure 2.

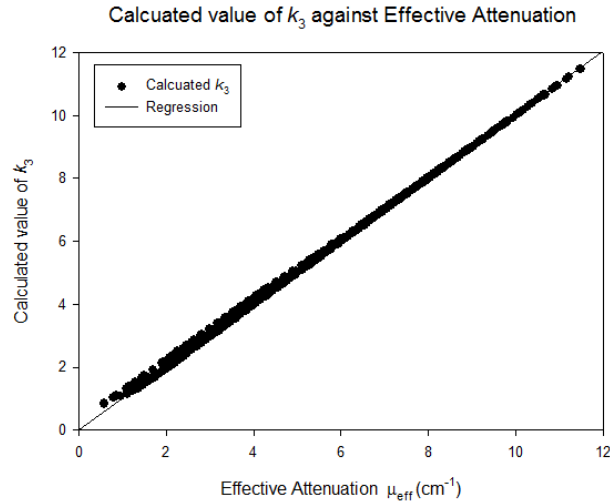


Figure 2) Relation between k_3 and μ_{eff}

It can be observed in Figure 2 that k_3 gives a good estimation of the value of effective attenuation coefficient μ_{eff} , which has a known relation with the absorption and reduced scattering coefficients. In other words, by measuring the first and second derivatives of the diffusion curve, the effective attenuation coefficient at a specific location can be estimated. In the next section, we will show how to apply the algorithm to obtaining the 2-D attenuation images.

III. 2-DIMENSIONAL ATTENUATION IMAGE

In our study, a commercially available CCD camera was used to record the 2-D diffuse reflectance profile on the area being scanned. The experimental setup is illustrated in Figure 3(a) and will be discussed in the following.

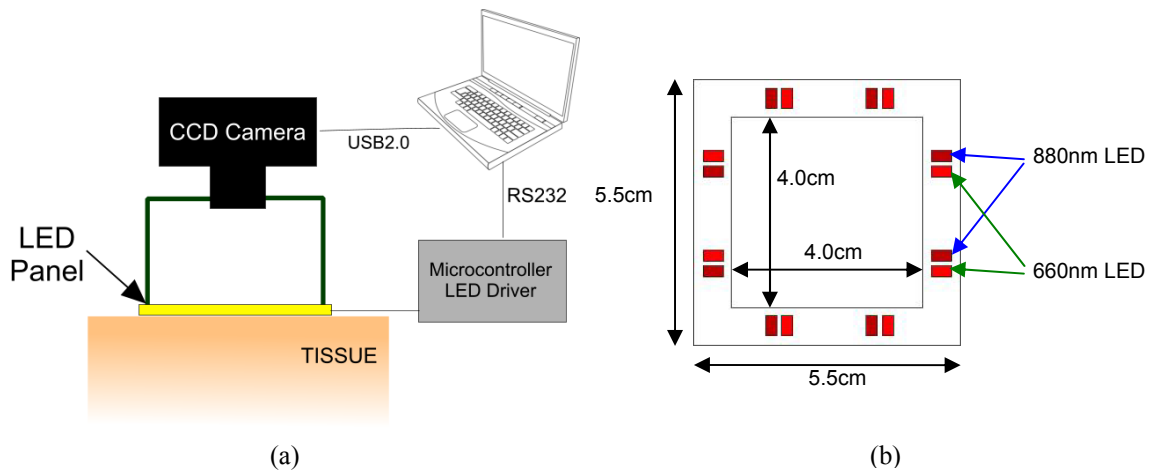


Figure 3) (a) Experimental setup; (b) Bottom view of LED panel.

A) System Architecture

The LED panel, composed of surface-mount-typed LEDs, is in direct contact with the subject under test. On top is a monochromic CCD camera (Mightex MCE-B013-U) which has a dynamic range over 80 dB. The lens attached to the

camera has a focal length of 5 mm. The camera is connected to a personal computer (PC) by USB 2.0 interface. The LEDs have central wavelength at either 660 or 880 nm, with a 3-dB spectral width of around 18 nm. They are controlled by a microcontroller unit through an LED driver IC. The PC connects to the microcontroller via RS232 interface. The program on the PC instructs the microcontroller to turn on the LEDs one by one. For each LED, several images are captured using the camera driver to control the exposure time and CCD amplification gain. Via the LED driver, the PC controls the input current to the LEDs. The captured images are then analyzed by the PC and the 2-D attenuation image is derived. The LED panel design is shown in Figure 3(b). Eight pairs of 660-nm and 880-nm LEDs are evenly distributed on the peripheral of the square ring board. With the effective distance of lumination of each LED around 2 to 3 cm, we are able to measure the diffuse reflectance on the whole area bounded by the square ring board of the LED panel. For each wavelength, 24 images are captures by turning on different LED and with different exposure time (3 exposure setting for each LED) as in figure 4 and 5. The captured images are then analyzed using the algorithm discussed in the previous section.

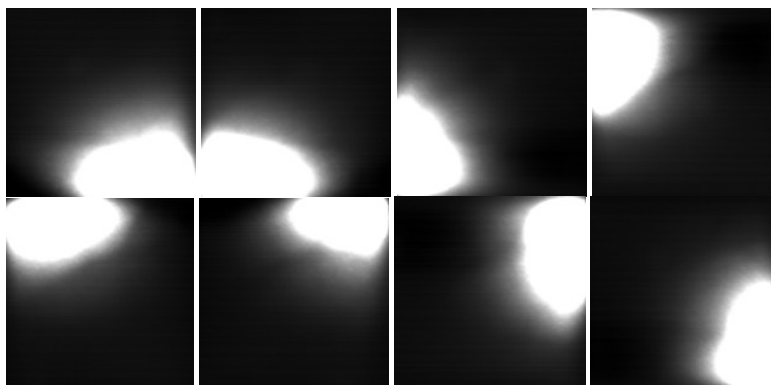


Figure 4. Captured images from 8 LEDs at different position.

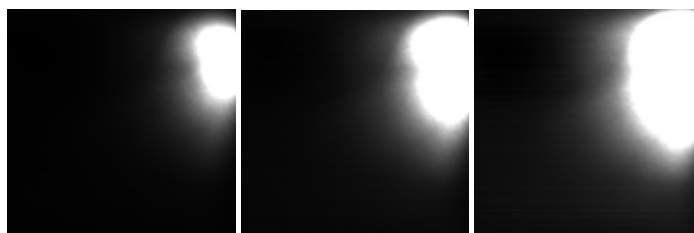


Figure 5. Captured images from LED number 7 with different exposure time

B) Experimental Results

The device was placed on the muscle of lower limbs of a volunteer. The captured images as in figure 4 and 5 were analyzed using the above algorithm and the resultant attenuation profile is shown in figure 6. The red color in the image represents the area with high attenuation value, while the blue color represents the area with low attenuation. The reconstructed 2-D attenuation image shows that there are two veins which are close to the skin surface. Venous blood contains high concentration of deoxygenated hemoglobin, leading to its high attenuation of red light. The values of μ_{eff}^2 computed for normal tissue (blue area) is around 8.26, whereas it is around 25.0 for the vein. The black color in the figure 6 indicates that the pixel readings of that particular point of all the images are not valid, due to low signal to noise ratio, and are discarded. The remedy to reduce the black area includes increasing the number of light sources, optimizing the placement of light source, and increasing the number of images captured with different exposures. The calculation result by the proposed algorithm apparently shows clearer details of the absorption profile for the whole area,

compared with the result in [6]. Compared with the previous spatially resolved technique, which can only give one set of optical parameters per probe, our resolved algorithm can give higher details of 2-D attenuation distribution.

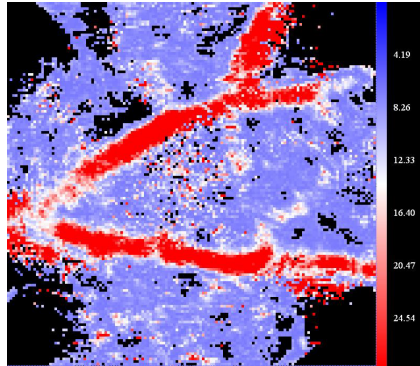


Figure 6. Resolved absorption coefficient on blood vessel under skin of wavelength 660nm

IV. CONCLUSION

We have proposed a novel scheme on the reconstruction of the attenuation profile based on reflectance curve measurement. We have shown that by calculating the local slope and the curvature of the reflectance curve, the local values of the attenuation coefficient can be obtained. With this technique, we are able to reconstruct the attenuation profile of non-homogenous medium. The scheme is successfully demonstrated in principle for the reconstruction of 2-D attenuation profile directly from the images captured by a CCD camera. It is demonstrated that optical parameters in high resolution can be obtained from the reflectance curve.

ACKNOWLEDGMENTS

This project is supported in part by an RGC Direct Grant of CUHK, 2009.

REFERENCES

1. H. Liu, Y. Song, K. L. Worden, X. Jiang, A. Constantinescu, R. P. Mason, "Noninvasive Investigation of Blood Oxygenation Dynamics of Tumors by Near-Infrared Spectroscopy", *Applied Optics*, Vol. 39, Issue 28, pp. 5231-5243 (2000)
2. T.J. Farrell, M.S. Patterson, B. Wilson, "A diffusion theory model of spatially resolved, steady-state diffuse reflectance for the noninvasive determination of tissue optical properties in vivo," *Med. Phys.* 19, 879-888(1992).
3. S.A. Prahl, M. Keijzer, S.L. Jacques, A.J. Welch, "A Monte Carlo model of light propagation in tissue," *Proc. SPIE* issue 5, 102-111 (1989)
4. D.E. Hyde, T.J. Farrell, M.S. Patterson, B.C. Wilson, "A diffusion theory model of spatially resolved fluorescence from depth-dependent fluorophore concentrations," *IOP Physic in Medicine and Biology* 46 (2001) 369-383.
5. L. Gobin, L. Blanchot, H. Saint-Jalmes, "Integrating the digitized backscattered image to measure absorption and reduced-scattering coefficients in vivo," *OSA Applied Optics* Vol. 38, No. 19 (1999)
6. K. J. Kek, R. Kibe, M. Niwayama, N. Kudo, K. Yamamoto, "Optical imaging instrument for muscle oxygenation based on spatially resolved spectroscopy," *Optical Express* 16, No.22, 18173-18187 (2008)
7. M.S. Patterson, B. Chance, B.C. Wilson, "Time resolved reflectance and transmittance for the non-invasive measurement of tissue optical properties," *OSA Applied Optics*, Vol. 28, No. 12 (1989)
8. W. Becker, A. Bergmann, G. Biscotti, A. Rück, "Advanced time-correlated single photon counting technique for spectroscopy and imaging in biomedical systems," *Proc. SPIE* (2004)
9. N.H. Kashou, R. Xu, C.J. Roberts, "Using fMRI and FNIRS for localization and monitoring of visual cortex activities", *IEEE EMBS* (2007)
10. M. Xu, H. Takata, S. Ge, T. Hayami, T. Yamasaki, S. Tobimatsu, K. Iramina, "NIRS Measurement of Hemodynamic Evoked Responses in the Primary Somatosensory Cortex by Finger Stimulation," *IEEE Conference on Complex Medical Engineering* (2007)